Lycopene cyclase paralog CruP protects against reactive oxygen species in oxygenic photosynthetic organisms

Louis M. T. Bradbury[a], Maria Shumskaya[a], Oren Tzfadia[a,b], Shi-Biao Wu[a], Edward J. Kennelly[a,b], and Eleanore T. Wurtzel[a,b,1]

[a]Department of Biological Sciences, Lehman College, City University of New York, West, Bronx, NY 10468; and [b]Graduate School and University Center, City University of New York, New York, NY 10016-4309

Edited by Rodney B. Croteau, Washington State University, Pullman, WA, and approved May 7, 2012 (received for review April 17, 2012)

In photosynthetic organisms, carotenoids serve essential roles in photosynthesis and photoprotection. A previous report designated CruP as a secondary lycopene cyclase involved in carotenoid biosynthesis [Maresca J, et al. (2007) P*roc Natl Acad Sci USA* 104:11784–11789]. However, we found that *cruP* KO or *cruP* overexpression plants do not exhibit correspondingly reduced or increased production of cyclized carotenoids, which would be expected if CruP was a lycopene cyclase. Instead, we show that CruP aids in preventing accumulation of reactive oxygen species (ROS), thereby reducing accumulation of β-carotene-5,6-epoxide, a ROS-catalyzed autoxidation product, and inhibiting accumulation of anthocyanins, which are known chemical indicators of ROS. Plants with a nonfunctional *cruP* accumulate substantially higher levels of ROS and β-carotene-5,6-epoxide in green tissues. Plants overexpressing *cruP* show reduced levels of ROS, β-carotene-5,6-epoxide, and anthocyanins. The observed up-regulation of *cruP* transcripts under photoinhibitory and lipid peroxidation-inducing conditions, such as high light stress, cold stress, anoxia, and low levels of CO_2, fits with a role for CruP in mitigating the effects of ROS. Phylogenetic distribution of CruP in prokaryotes showed that the gene is only present in cyanobacteria that live in habitats characterized by large variation in temperature and inorganic carbon availability. Therefore, CruP represents a unique target for developing resilient plants and algae needed to supply food and biofuels in the face of global climate change.

photoinhibition | stress tolerance | chilling stress | oxygenic photosynthesis

Carotenoids are C_{40} compounds found in a wide variety of organisms, where they play important roles in photoprotection and light harvesting (1). In photosynthetic organisms, carotenoids with cyclic end groups are essential for light harvesting (2, 3). Lycopene, a linear carotenoid, is the major branch point for the formation of different cyclic carotenoids, such as α-carotene or β-carotene (4). The cyclization of the ends of lycopene is performed by a class of enzymes known as lycopene cyclases (5–8). In plants, the enzymatic products of the CrtL type lycopene cyclases, lycopene ε-cyclase (LCYE) and lycopene β-cyclase (LCYB), are α-carotene and β-carotene. These carotenoids can be hydroxylated to generate lutein and zeaxanthin, respectively. Lutein functions in the assembly of the photosystems and plays a role, together with zeaxanthin, in light harvesting within the antenna of photosystems I and II (PSI and PSII) (9). β-carotene found in the reaction center of PSII has a protective role, quenching singlet oxygen generated during the water-splitting process of photosynthesis (10, 11).

Various structural types of lycopene cyclases have been identified in carotenogenic organisms, such as the CrtL type found in plants, algae, and some cyanobacteria (5, 12, 13); the CrtY type in flavobacteria (14); and a heterodimeric type found in some Gram-positive bacteria and fungi (7, 15, 16). Recently a fourth family of lycopene cyclases was identified in green sulfur bacteria (GSB) and some cyanobacteria (8). This previously undescribed family of lycopene cyclases is composed of two classes of enzymes, one known as CruA (found in all GSB and cyanobacteria that lack CrtL) and a paralog known as CruP found in cyanobacteria, along with CruA or CrtL, and in higher plants along with CrtL enzymes (LCYB and LCYE).

In *Escherichia coli* complementation assays, CruA from the GSB *Chlorobium tepidum* ($_{Ct}$CruA) was shown to convert lycopene into γ-carotene plus small amounts of β-carotene (8). The cyanobacterial *Synechococcus* sp. *PCC 7002* CruP ($_{Syn}$CruP) was also shown to convert lycopene into γ-carotene but had lower activity than $_{Ct}$CruA (8). In general, carotenoid biosynthesis in plants and cyanobacteria is performed by a similar suite of enzymes. Although plants already contain two CrtL type lycopene cyclases that form β- and ε-rings, Maresca et al. (8) suggested that CruP in plants might be a lycopene cyclase specifically responsible for catalyzing formation of β-rings of α-carotene (8). However, the pigment profile of both the *Synechococcus* sp. *PCC 7002* and the *Synechocystis* sp. *PCC 6803 cruP* KOs was phenotypically identical to that of WT (8, 17), which is unexpected if CruP is indeed a lycopene cyclase.

Results

Functional Analysis of $_{Syn}$CruP. To confirm published reports that $_{Syn}$CruP is a lycopene cyclase (8), we expressed both $_{Syn}$*cruP* and *cruA* from *Chlorobium phaeobacteroides* ($_{Cp}$*cruA*) in *E. coli* BL21 containing pAC-CRT-EIB, which confers lycopene accumulation. In this system, a functional lycopene β-cyclase converts lycopene into γ-carotene or β-carotene. However, expression of pET16-$_{Syn}$CruP in this lycopene-accumulating strain of *E. coli* revealed that despite high production of CruP protein (Fig. S1), there was no change in the pigments produced in comparison to a strain containing pAC-CRT-EIB and the empty pET16b vector (Fig. 1 *A* and *B*). In contrast, expression of p16-CPL1 containing $_{Cp}$CruA led to conversion of all the lycopene into γ-carotene (Fig. 1*C*). Therefore, only CruA, and not CruP, appeared to have lycopene cyclase activity in *E. coli*.

***Zea mays* CruP Protein Subcellular Localization.** If CruP is a lycopene cyclase, it should be localized to chloroplasts, the site of carotenoid biosynthesis. We therefore tested the location of *Zea mays* CruP ($_{Zm}$CruP) in chloroplasts via in vitro import experiments. Incubation of $_{Zm}$CruP with isolated pea chloroplasts led to im-

Author contributions: L.M.T.B. and M.S. designed research; L.M.T.B., M.S., and S.-B.W. performed research; L.M.T.B., M.S., O.T., S.-B.W., E.J.K., and E.T.W. analyzed data; and L.M.T.B., M.S., and E.T.W. wrote the paper.

The authors declare no conflict of interest.

This article is a PNAS Direct Submission.

[1]To whom correspondence should be addressed. E-mail: wurtzel@lehman.cuny.edu.

See Author Summary on page 10767 (volume 109, number 27).

This article contains supporting information online at www.pnas.org/lookup/suppl/doi:10.1073/pnas.1206002109/-/DCSupplemental.

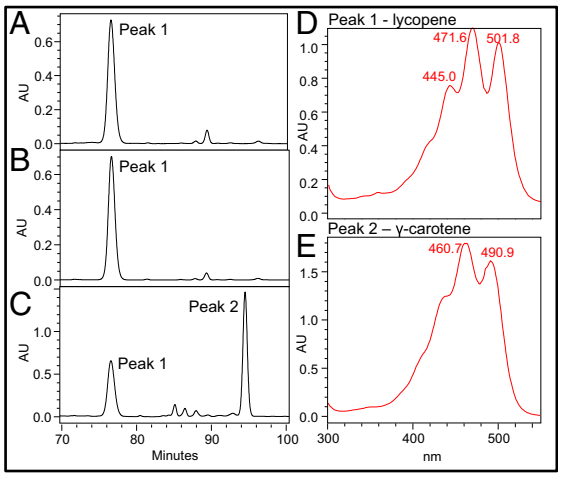

Fig. 1. HPLC analysis of carotenoids extracted from *E. coli* BL21 cells containing pAC-CRT-EIB and empty pET16b vector (*A*), pET-$_{Syn}$CruP (*B*), and p16-CPL1 (*C*; $_{cp}$CruA). The absorbance spectrum of peak 1 (*D*; lycopene) and peak 2 (*E*; γ-carotene) is also shown. AU, absorbance units.

port and processing of the $_{Zm}$CruP precursor protein (large band in Fig. 2*A*, P) to generate a smaller mature protein (smaller band in Fig. 2*A*, I). After thermolysin treatment of the chloroplasts (Fig. 2*A*, T), only the smaller protein remained, showing that the mature protein is completely inside the chloroplast and is protected by the outer membrane. Fractionation of chloroplasts not treated with thermolysin showed that $_{Zm}$CruP is present in the membrane fraction (Fig. 2*A*, M) and is absent from the soluble fraction (Fig. 2*A*, S). After alkaline treatment (Fig. 2*A*, A), the membrane fraction was devoid of $_{Zm}$CruP, showing that it is a peripherally membrane-bound chloroplast protein. Chloroplast localization of $_{Zm}$CruP was further corroborated by transient expression in maize leaf protoplasts using a $_{Zm}$CruP:GFP fusion driven by a 35S promoter. The GFP fluorescence of the fusion protein localized with chlorophyll fluorescence (Fig. 2*B*). Therefore, the import and transient expression experiments demonstrate chloroplast localization of $_{Zm}$CruP. The precise suborganellar location is likely to be thylakoids, as suggested by proteomic surveys conducted in *Arabidopsis* (The Plant Proteome Database; http://ppdb.tc.cornell.edu/dbsearch/searchsample.aspx).

***In Silico* Analysis of CruP Expression.** To gain further insight into the function of CruP, we compared $_{At}$*cruP* gene expression with expression of other genes encoding carotenoid enzymes in *Arabidopsis*. The expression profile of $_{At}$*cruP* analyzed using Genevestigator showed that $_{At}$*cruP* is expressed highest in green tissues (e.g., pedicels, sepals, cotyledons, young leaves). $_{At}$*cruP* is up-regulated by light as seen for carotenoid-related genes (18). However, in contrast to most carotenoid-related genes, $_{At}$*cruP* is expressed at relatively low levels under most conditions except cold stress and dark anoxic treatment, where $_{At}$*cruP* is highly expressed (Tables 1 and 2). Most other stress stimuli data available on Genevestigator, including drought and abscisic acid (ABA) treatment, either do not alter expression or decrease expression of $_{At}$*cruP*. Therefore, transcript levels of CruP appear to be controlled independent of carotenoid pathway genes, which would be consistent with a role of CruP distinct from carotenogenesis.

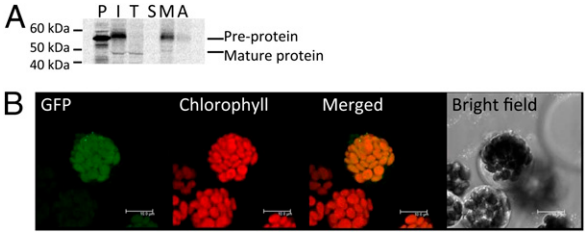

Fig. 2. Localization of $_{Zm}$CruP in chloroplasts. (*A*) Signal detected from SDS/PAGE gel of radiolabeled $_{Zm}$CruP before (P) and after (I) import into chloroplasts. A, alkaline-treated membrane fraction; M, membrane fraction; S, soluble fraction; T, thermolysin-treated fraction. (*B*) Transient expression of $_{Zm}$CruP:GFP under a 35S promoter in bean cotyledon protoplasts showing GFP fluorescence and chlorophyll fluorescence, a merged image showing both GFP and chlorophyll fluorescence, and a bright-field image showing intact protoplast.

In Vivo Analysis of CruP from Higher Plants. Photosynthetic organisms that lack lycopene cyclase activity exhibit accumulation of lycopene along with aberrant chloroplast ultrastructure (19), which appears not to be the case for *cruP* mutants. Previous reports of phenotypes from *cruP* KOs in cyanobacteria range from no phenotype (8) to descriptions of disordered thylakoid membranes (17). In both cases, no change in carotenoid pigment profile was observed. To test whether plant mutants of CruP might exhibit evidence of lycopene cyclase activity, we analyzed *cruP* KO and overexpressing *Arabidopsis* plants. RT-PCR confirmed an absence of $_{At}$*cruP* transcripts in the KO line (SALK_011725) (20) and overexpression of $_{Zm}$*cruP* transcripts in the four *35S:*$_{Zm}$*cruP* transgenic lines (Fig. S2). We noted that the growth rate of the KO plants was significantly slower than that of the WT plants (Fig. 3). At 2 wk of growth on MS medium, WT plants had, on average, seven leaves, whereas KO plants had, on average, only four leaves. The pigment profile of the KO plants showed no change in levels of lutein (the hydroxylation product of α-carotene), suggesting CruP was not involved in the production of α-carotene, as had been previously suggested (8). The only consistent difference observed was that of a small peak barely noticeable in the WT, which was found to be present at levels roughly 10-fold higher in the $_{At}$*cruP* KO plants (Fig. 4).

To confirm that the presence of the unknown peak was not attributable to another random mutation within this KO line, a segregating population was obtained by crossing the KO line with the Columbia WT, followed by selfing of the progeny. Eight homozygous KOs obtained from this cross were analyzed by HPLC, and all were found to contain the unknown peak (Fig. 5*C*). In contrast, this peak was virtually absent in all seven of the analyzed WT plants generated from this cross (Fig. 5*A*). Three heterozygous plants were also analyzed and showed half as much of the unknown peak as the homozygous KO plants (Fig. 5*B*). We also crossed lines to produce plants that were heterozygous for the $_{At}$*cruP* KO and hemizygous for *35S:*$_{Zm}$*CruP*; the pigment profile of these plants was examined and showed complete absence of the unknown peak (Fig. 5*D*).

Table 1. Carotenoid gene transcripts up-regulated more than 1.5-fold by chilling stress

Carotenoid		20 °C,	4 °C,	Fold up-regulated
Protein	Gene	average	average	at 4 °C
NCED5	AT1G30100	3.79	20.79	5.48
CruP	AT2G32640	27.16	120.69	4.44
CYP97C	AT3G53130	95.99	250.04	2.60
HYD2	AT5G52570	88.97	166.32	1.87
ZEP	AT5G67030	871.64	1,508.78	1.73
LYCE	AT5G57030	208.46	344.07	1.65
CCD7	AT2G44990	25.13	39.42	1.57

Data obtained from published microarray data available via Genevestigator. CruP highlighted in green.

Table 2. Carotenoid gene transcripts up-regulated more than 1.5-fold by anoxia

Carotenoid		Air,	No air,	Fold up-regulated
Protein	Gene	average	average	under dark anoxia
CruP	AT2G32640	22.8	49.45	2.17
ZEP	AT5G67030	87.95	159.4	1.81
CCD8	AT4G32810	33.9	59	1.74
CCD1	AT3G63520	241.8	407.7	1.69
NCED9	AT1G78390	0.6	0.95	1.58
HYD2	AT5G52570	37.6	57.75	1.54

Data obtained from published microarray data available via Genevestigator. CruP highlighted in green.

The retention time of the unknown peak was of a carotenoid that was more polar than α-carotene and β-carotene but less polar than α-cryptoxanthin and β-cryptoxanthin (monohydroxylated carotenes). The spectrum (Fig. 5*E*) suggested that this compound had fewer conjugated double bonds than β-carotene. A study of the literature for rare carotenoids found in plants provided many possibilities (21–24), but none seemed more likely than β-carotene-5,6-epoxide, a carotenoid that has previously been observed in photosynthetic tissues (21). β-carotene-5,6-epoxide was synthesized (25) and subjected to HPLC analysis, where it eluted at the same time and with the same spectrum as the unknown carotenoid (Fig. 6). Additional liquid chromatography (LC)-MS analysis of the peak from the KO plant confirmed a major ion fragment with a mass of 553 $[M+H]^+$, corresponding to the mass of β-carotene-5,6-epoxide (Fig. S3).

Because $_{At}$*cruP* transcripts are up-regulated at low temperatures (Tables 1 and 2), $_{At}$*cruP* KO plants were grown at 4 °C to observe the impact on levels of β-carotene-5,6-epoxide. Growth of both KO and WT plants at 4 °C for 10 d led to an increase in β-carotene-5,6-epoxide in both plants relative to plants grown at 21 °C (Fig. 7). A slight decrease in β-carotene was also observed in the $_{At}$*cruP* KO plant in comparison to the WT plant (Fig. 7). This decrease in β-carotene was approximately equivalent to the increase in β-carotene-5,6-epoxide. At 4 °C, there was much more variation in β-carotene levels in both the $_{At}$*cruP* KO and WT plants, but a decrease in β-carotene was still observed in the $_{At}$*cruP* KO plants (Fig. 7).

Reactive Oxygen Species. Considering published reports of β-carotene-5,6-epoxide formation via reactive oxygen species (ROS)-mediated degradation of β-carotene in photosynthetic tissues exposed to high light stress (21), together with our own observations of β-carotene-5,6-epoxide accumulation in $_{At}$*cruP* KO plants and up-regulation of *cruP* in ROS-producing conditions (cold stress and dark anoxic treatment), we considered that CruP may play a role in reducing the accumulation of ROS. Cotyledons from Columbia (WT), $_{At}$*cruP* KO, and *35S:*$_{Zm}$*cruP* lines exposed to anoxic conditions for 1 wk were stained with nitrotetrazolium blue (NTB) to screen for levels of ROS (Fig. 8). WT plants showed partial staining, whereas $_{At}$*cruP* KO plants showed staining throughout the entire cotyledon. *35S:*$_{Zm}$*cruP* lines showed minimal to no staining in comparison to the WT plants. These results clearly demonstrate that ROS levels in cotyledons are inversely correlated with CruP transcript levels. To investigate the connection between CruP and stress responses further, WT Columbia, $_{At}$*cruP* KO, and three *35S:*$_{Zm}$*CruP* lines were grown for 1 mo under standard conditions at 21 °C before being transferred to 4 °C with continuous light (50 $\mu mol \cdot m^{-2} \cdot s^{-1}$) for 2 mo. This cold stress treatment revealed a striking difference between plants that differed only in CruP levels. Columbia and $_{At}$*cruP* KO plants developed deep anthocyanin staining throughout the entire plant, whereas the three overexpressor *35S:*$_{Zm}$*CruP* lines remained a deep green color with minimal or no anthocyanin development (Fig. 9). The anthocyanin response is consistent with increased ROS in the WT and KO plants and decreased ROS in the overexpression lines.

Coexpression Analysis of CruP. Coexpression analysis of genes encoding $_{At}$CruP and $_{At}$LCYE (Dataset S1) showed that the majority of coexpressed genes encode proteins involved in chlorophyll biosynthesis, photosystem repair, or other photosynthesis-related functions. Photosynthesis-related genes that were coexpressed with $_{At}$*cruP* but not $_{At}$*lcyE* included many genes involved in protection of PSII against oxidative damage as well as those involved in repair of PSII after damage by singlet oxygen. Such genes include those encoding thioredoxins; HCF136; the PSII reaction center D1 proteases DEG8 (26) and FtsH5 (also known as VAR1) (27); SVR3, which is important for chloroplast development in cold conditions, mutants of which suppress variegation in *var2* mutants (28); and PPL1 involved in PSII repair (29). Other notable coexpressed genes include *cch1-1* (*gun5*), which is involved in generating a putative plastid-to-nucleus signal in response to high light stress (30), as well as genes encoding dicarboxylate transporters DIT1 and DIR2, mutants of which require high CO_2 for survival (31); a ribose 5-phosphate isomerase involved in CO_2 fixation (32); and a YfhF homolog involved in inhibiting chloroplast division (33) (Dataset S1*A*). Many of these genes were also coexpressed with the gene encoding CruP from *Oryza sativa* ($_{Os}$CruP) (Dataset S1*B*). Chlorophyll-related genes that were coexpressed with the gene encoding $_{At}$LCYE but not $_{At}$CruP include four genes encoding proteins that are part of the NAD(P)H dehydrogenase complex that is involved in cyclic electron transfer around PSI (34, 35), as well as genes that encode proteins involved in chlorophyll synthesis (e.g., protochlorophyllide reductase) and chlorophyll binding proteins of PSI and PSIII (e.g., chlorophyll A-B binding protein) (Dataset S1*C*). Another gene of note is *ftsZ*, encoding a chloroplast division protein that functions antagonistically with the YfhF homolog mentioned above (33).

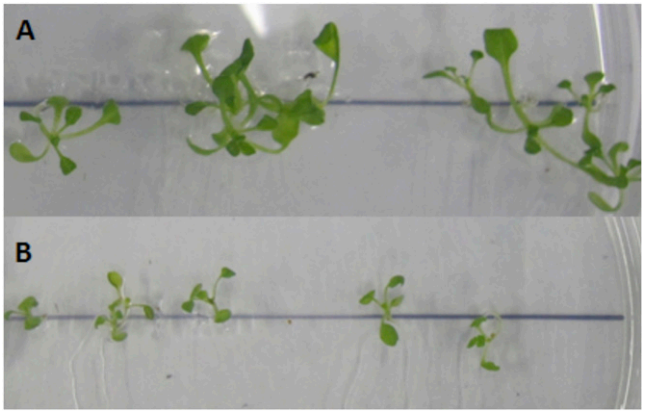

Fig. 3. Two-week-old plants grown on MS media. Columbia WT (*A*) and $_{At}$*cruP* KO (*B*).

Phylogenetic Distribution. Previous reports of CruP showed distribution of the gene in higher plants and some cyanobacterial species. To determine how important CruP is for fitness in photosynthetic organisms, we performed a BLAST analysis to determine the distribution of CruP more thoroughly. A protein BLAST analysis of CruP from *Synechococcus* sp. *PCC 7002* revealed that CruP orthologs are only found in oxygenic photosynthetic organisms. These organisms encompass various families, such as cyanobacteria, green and brown algae, diatoms, mosses, and higher plants, including both monocots and dicots. An analysis of CruA orthologs showed that as well as being found in oxygenic

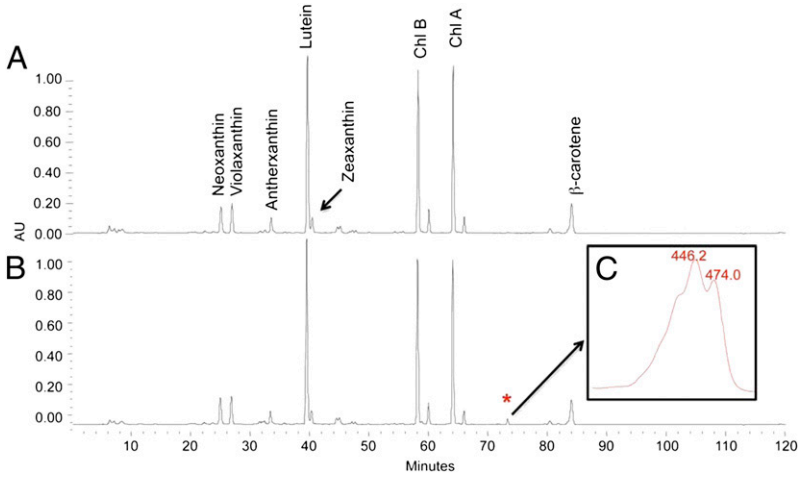

Fig. 4. HPLC analysis of carotenoids extracted from *Arabidopsis* plants. Columbia WT (*A*) and $_{At}$*cruP* KO (*B*), and absorbance spectra of the unique peak (*) identified in the $_{At}$*cruP* KO plants (*C*). AU, absorbance units.

cyanobacteria that lack CrtL type cyclases, CruA was present in nonoxygenic organisms, such as Chlorobi, Chloroflexi, and delta-proteobacteria. A protein BLAST analysis of CrtL from the cyanobacterium *Synechococcus elongatus PCC 6301* showed that CrtL orthologs were scattered throughout various species and are by no means isolated to oxygenic photosynthetic organisms, as in the case of CruP (Table 3 and Dataset S2).

A phylogenetic tree (Fig. 10) was constructed using 16S rRNA sequences of fully sequenced cyanobacteria and mitochondrial 16S rRNA of *Arabidopsis thaliana* as an outlier. The tree revealed that those cyanobacteria that do not contain CruP belong to a distinct clade. Further BLAST analysis was undertaken using CsoS2 and CcmN, proteins involved in CO_2-concentrating mechanisms of distinct cyanobacterial groups, known as α-cyanobacteria and β-cyanobacteria, respectively (36). The results revealed that β-cyanobacteria contain CruP, whereas α-cyanobacteria do not. Two exceptions were noted, *Thermosynechococcus elongatus BP-1* and *cyanobacterium UCYN-A*, which are β-cyanobacteria but do not contain CruP. The reason for this presence or absence of CruP in the separate groups is likely attributable to the different environments inhabited by these organisms. Hints as to the precise environmental factor(s) that influence the presence or absence of CruP might be gleaned from *T. elongatus* and *cyanobacterium UCYN-A*, two β-cyanobacteria that do not contain CruP (*Discussion*).

Genes That Cluster with Cyanobacterial CruP. In bacteria, genes involved in similar processes are often found clustered in the genome. We determined what genes tend to cluster with *cruP* in select cyanobacterial genomes to see if we could infer function of CruP. Analysis of genes that cluster with *cruP* revealed genes with functions similar to those of genes that are found to be coexpressed with $_{At}$*cruP* and $_{Os}$*cruP*. Examples include genes encoding proteins with roles related to PSII D1 degradation, such as YP_001733313, an FtsH5 homolog in *Synechococcus* sp. *PCC 7002*, and the ClpC

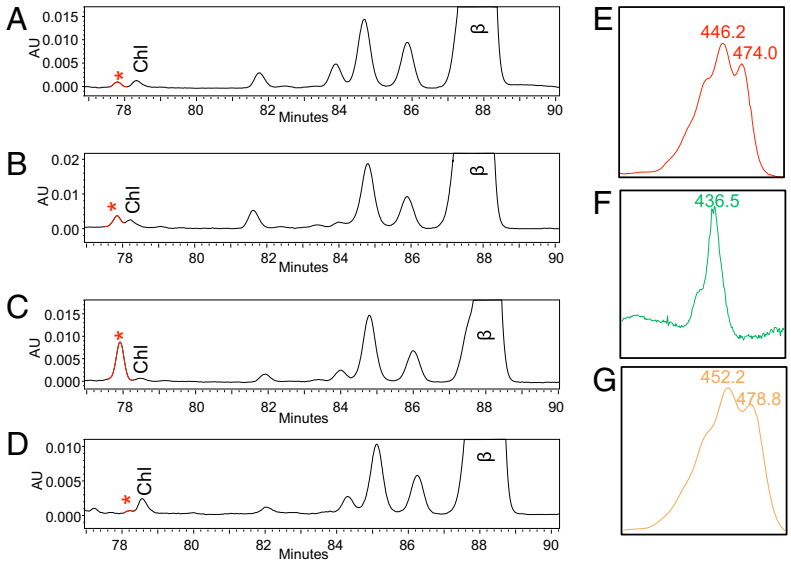

Fig. 5. HPLC analysis of carotenoids extracted from a segregating population of *Arabidopsis* plants. Typical homozygous WT plant (*A*), typical heterozygous $_{At}$*cruP* KO plant (*B*), typical homozygous $_{At}$*cruP* KO plant (*C*), and typical heterozygous $_{At}$*cruP* KOt/hemizygous *35S:*$_{Zm}$*CruP* plant (*D*). Absorbance spectra of the unique peak (*) identified in the $_{At}$*cruP* KO plants (*E*), absorbance spectra of the unknown chlorophyll-like peak (*F*; Chl), and absorbance spectra of β-carotene (*G*; β). Unknown cis-carotenoids were also observed to elute between Chl and β. AU, absorbance units.

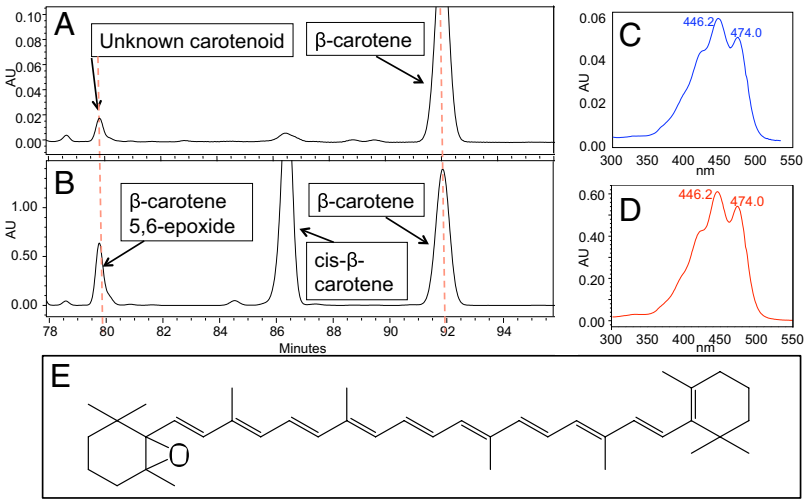

Fig. 6. Comparison of HPLC elution profiles of pigments extracted from a homozygous $_{At}$*cruP* KO plant (*A*) to a synthesized β-carotene-5,6-epoxide standard (*B*). (*C*) Absorbance spectra of the unknown peak from the $_{At}$*cruP* KO plants. (*D*) Absorbance spectra of the synthesized β-carotene-5,6-epoxide standard. (*E*) Chemical structure of β-carotene-5,6-epoxide. AU, absorbance units.

(NP_925429, YP_478720) and ClpB (YP_473669) proteases in *Gloeobacter violaceus PCC 7421*, *Synechococcus* sp. *JA-2-3B'a* (*2-13*), and *Synechococcus* sp. *JA-3-3Ab* (Fig. 11). The genes encoding the PSII reaction center proteins D2 (YP_399674) and CP43 (YP_399675) of *S. elongatus PCC 7942* are also clustered near *cruP*, as are the genes encoding YP_001867515, a RuBisCO small subunit protein in *Nostoc punctiforme PCC 73102*, and YP_003721373, encoding a CO_2-concentrating mechanism protein known as CcmK in *Nostoc azollae 0708* (Fig. 11). Orthologs of many of the genes that cluster with *cruP* in different cyanobacteria were found coexpressed with both $_{At}$*cruP* and $_{Os}$*cruP* and are important in oxygenic photosynthetic organisms under cold stress and low CO_2, suggesting that CruP is involved in the same process in cyanobacteria as it is in plants.

Discussion

CruP Is a Chloroplast Protein but Does Not Exhibit Lycopene Cyclase Activity. Although Maresca et al. (8) observed lycopene cyclase activity from $_{Syn}$CruP in *E. coli*, we were not able to replicate their results despite obtaining ample expression levels of the $_{Syn}$CruP protein (Fig. S1). We were able to replicate cyclase activity of $_{Cp}$CruA. Although the differences observed between our results and those of Maresca et al. (8) could be attributable to *E. coli* strain differences or differences in growth conditions, we did try multiple *E. coli* strains and growth conditions, all with identical results (i.e., no cyclization of lycopene was observed). The finding that CruP is a peripheral thylakoid membrane protein in chloroplasts suggested the possibility of another chloroplast-localized role.

CruP, β-Carotene-5,6-Epoxide, and ROS. We identified β-carotene-5,6-epoxide in the pigment profile of *Arabidopsis cruP* KO plants at levels substantially higher than those found in WT or *35S:*$_{Zm}$*cruP* plants. The increase of β-carotene-5,6-epoxide in the $_{At}$*cruP* KO plants coincided with an approximate equivalent decrease in β-carotene levels (Fig. 7). The level of β-carotene-5,6-epoxide was observed to increase in the $_{At}$*cruP* KO plants in response to chilling

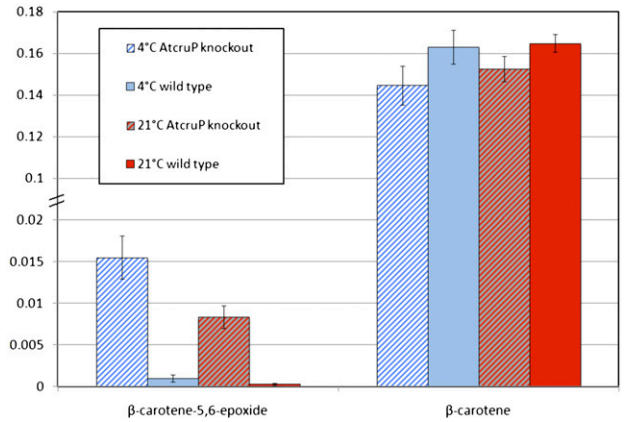

Fig. 7. Levels of β-carotene and β-carotene-5,6-epoxide displayed as a ratio of total chlorophyll from leaves of *Arabidopsis* plants (Columbia WT and $_{At}$*cruP* KO) grown under different temperatures.

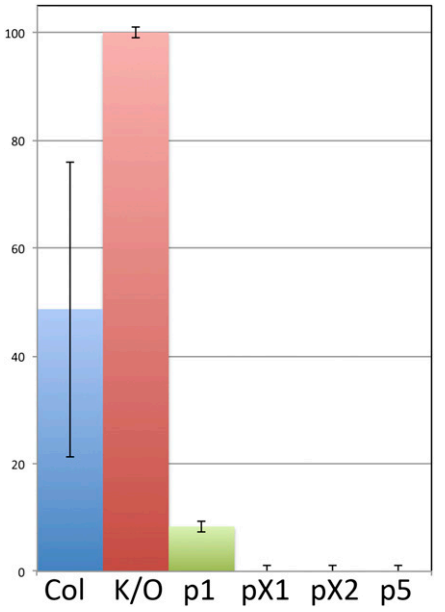

Fig. 8. ROS levels in cotyledons shown as a percent area of cotyledons stained by NTB. Lines used are Columbia WT (Col); CruP KO (K/O); and 35S: ZmCruP lines p1, pX1, pX2, and p5.

Fig. 9. *Arabidopsis* plants shifted to 4 °C with continuous light for 2 mo show production of (or lack of) anthocyanin in response to this stress. Columbia WT (*A*); $_{At}$*cruP* KO (*B*); and *35S:*$_{Zm}$*cruP Arabidopsis* plants pX1, pX2, and p5 (*C*–*E*), respectively.

stress (Fig. 7), a condition known to up-regulate $_{At}$*cruP* transcripts (Table 1). β-carotene-5,6-epoxide has been identified in intact and isolated thylakoid membranes of spinach and *T. elongatus* (21). The level of β-carotene-5,6-epoxide in thylakoid membranes of spinach increased in proportion to light intensity. In a study of the protective role of β-carotene in photosystems (37), isolated bacteriochlorophyll and β-carotene dissolved in oxygenated acetone were exposed to light and chlorophyll molecules were observed to be protected at the expense of β-carotene. The first product formed in this reaction was β-carotene-5,6-epoxide, followed by progressively more oxygenated β-carotene products. Oxidation of carotenoids by singlet oxygen is an unavoidable consequence of oxygenic photosynthesis. This oxidation is especially true of β-carotene, which is the only carotenoid found in the core of PSII, the site of the water-splitting/oxygen-evolving complex (10, 38). The main role of β-carotene in the reaction center is quenching of singlet oxygen (10, 11, 39). Bleaching of this β-carotene by singlet oxygen has been proposed to trigger turnover of the D1 protein in the PSII reaction center (40). We showed that the absence of CruP was associated with increased ROS and increased β-carotene-5,6-epoxide, whereas the overexpression of CruP was associated with reduced ROS and reduced β-carotene-5,6-epoxide (Figs. 5 and 8). The impact of CruP overexpression on anthocyanin production, a known ROS response, in cold-treated plants was quite striking in comparison to WT and CruP KO plants (Fig. 9). WT and CruP KO plants both showed accumulation of large amounts of anthocyanins under this stress condition, whereas the overexpressors remained green and healthy. Anthocyanin accumulation is a well-characterized response of plants to increased ROS production, again showing the impact of CruP activity on ROS levels in plants treated under photoinhibitory conditions.

***cruP* Transcripts Are Up-Regulated in Response to Photoinhibition.** *In silico* analysis revealed that *A. thaliana cruP* is up-regulated under chilling stress and dark anoxia (Tables 1 and 2). Cotyledons and pedicels, where CruP transcripts were shown to be elevated, have been shown to undergo photoinhibition stress and high singlet oxygen production under normal "nonphotoinhibitory" conditions, in comparison to true leaves (41, 42). Chilling stress in plants causes a range of physiological effects similar to those observed under high light stress (e.g., 43, 44). In addition, cold stress causes inhibition of the PSII D1 repair mechanism as a result of decreased membrane fluidity (45), leading to further increases of ROS. Dark anoxic treatment of plants leads to generation of nitric oxide and also, paradoxically, to increased levels of ROS, including super oxide anions and hydrogen peroxide (46, 47). Dark anoxia for prolonged periods causes peroxidation of lipid membranes (47). A recent analysis of the expression of all known carotenoid synthesis genes in *Synechococcus* sp. *PCC 7002* showed that despite the fact that "transcript levels for genes encoding enzymes producing γ- and β-carotene from geranylgeranyl-pyrophosphate were generally much lower under anoxic conditions," *cruP* is, in fact, up-regulated greater than 10-fold under dark anoxic conditions and is up-regulated greater than threefold by low CO_2 conditions, whereas *cruA* is down-regulated twofold under both of these photoinhibitory/singlet oxygen-producing conditions (48). All these conditions and tissues, in which *cruP* transcript levels are elevated, are observed to have increased ROS production in comparison to true photosynthetic tissues and optimal growth conditions.

Coexpression and Clustering of CruP with PSII-Related Protection Mechanisms. Coexpression analysis of $_{At}$*cruP* revealed that $_{At}$*cruP* was coexpressed with genes that code for proteins that function in the protection or repair of PSII from oxidative damage (e.g., the D1 proteases FtsH5 and DEG8) or proteins involved in prevention of photoinhibition (e.g., those involved in inorganic carbon transport and fixation as well as chloroplast development in cold conditions). Cyanobacterial *cruP* genes were clustered with genes of the PSII reaction center and with genes involved in the repair of oxidatively damaged PSII reaction center proteins (e.g., FtsH5, ClpC, ClpB), as well as with those involved in carbon acquisition and fixation. This gene clustering pattern fits with the observation that *cruP* transcripts are up-regulated in both *Arabidopsis* and *Synechococcus* sp. *PCC 7002* under photoinhibitory/ROS-producing conditions, such as low CO_2 and chilling stress. In contrast, the gene encoding $_{At}$LCYE was coexpressed with genes involved in chlorophyll synthesis and photosystem assembly as well as *ftsZ*, a gene involved in chloroplast division that functions antagonistically with *yfhF* (a gene coexpressed with *cruP*) (Dataset S1). The observed coexpression

Table 3. Phylogenetic distribution of CruA, CrtY, and CrtL type cyclases and CruP protein

	Family	CrtY	CrtL	CruA	CruP	Photosynthetic?
Prokaryotic	Deinococcus-Thermus	One	Most	None	None	Nonphotosynthetic
Prokaryotic	Actinobacteria	Some	Most	None	None	Nonphotosynthetic
Prokaryotic	Bacteriodetes non-Chlorobi	All	None	None	None	Nonphotosynthetic
Prokaryotic	Chlorobi (GSB)	None	None	All	None	Nonoxygenic photosynthesis
Prokaryotic	Chloroflexi	Some	Some	One	None	Nonoxygenic photosynthesis
Prokaryotic	Proteobacteria	Mostly	One	One	None	Nonphotosynthetic
Prokaryotic	Cyanobacteria	None	Some	Some	Some	Oxygenic photosynthesis
Eukaryotic	Viridiplantae	None	All	None	All	Oxygenic photosynthesis
Eukaryotic	Stramenophiles	None	All	None	All	Oxygenic photosynthesis

Highlighted in green are oxygenic photosynthetic organisms (note that this covers the range of cruP containing organisms). Nonoxygenic photosynthetic organisms are highlighted in yellow.

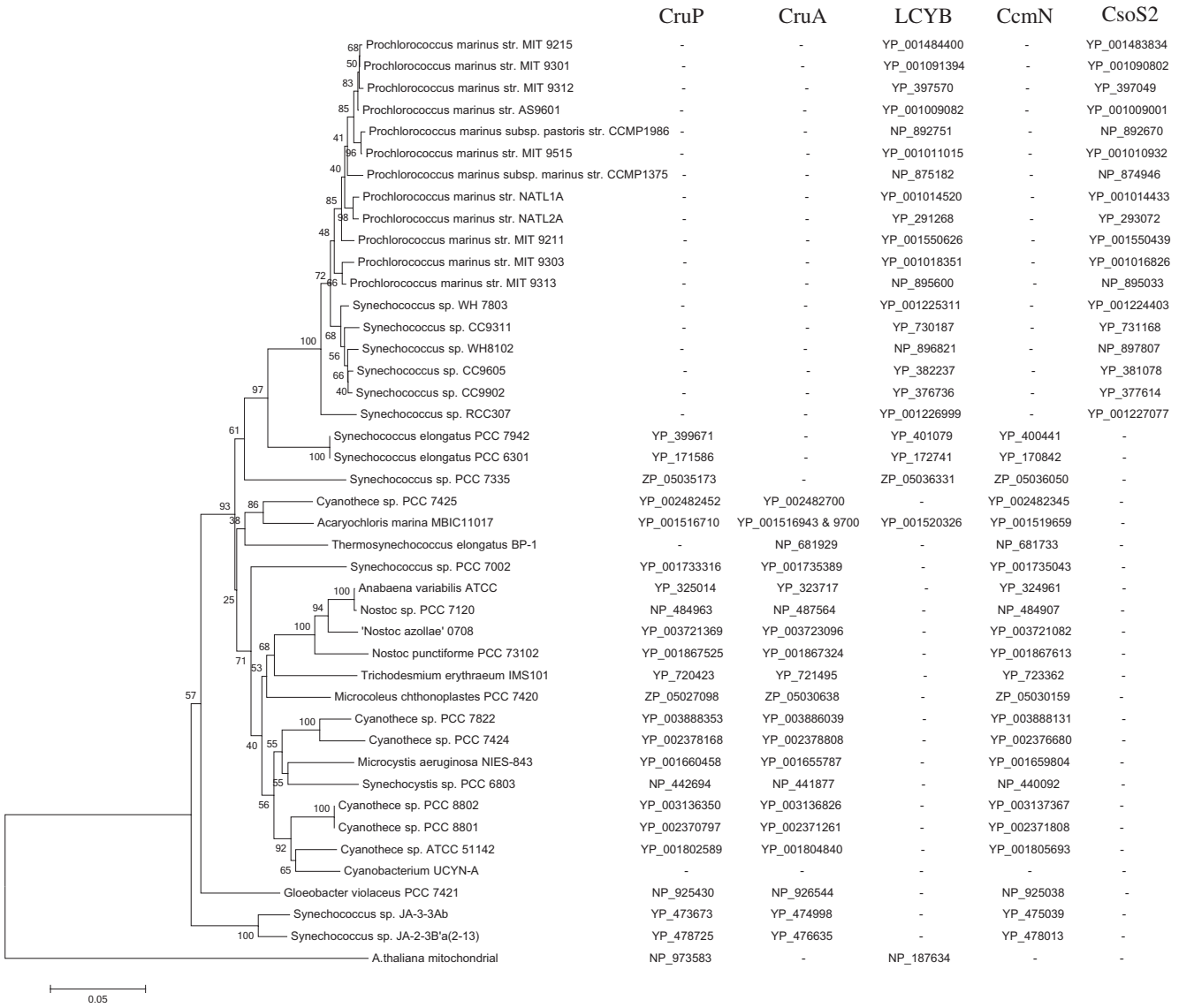

Fig. 10. Phylogenetic tree based on 16S rRNA sequences of completely sequenced cyanobacteria using *A. thaliana* mitochondrial 16S rRNA as an outlier. Bootstrap values shown are based on 1,000 replicates. Columns to the right of the tree show the GenBank protein accession numbers of CruP, CruA, LCYB, CcmN, or CsoS2 if it is present in that organism.

pattern suggests differing roles for LCYE and CruP in growth and protection from oxidative damage, respectively.

CruP Was Found Only in Oxygenic Photosynthetic Organisms. Although all other lycopene cyclases are found in a wide variety of organisms, both oxygenic and nonoxygenic phototrophs as well as nonphotosynthetic organisms, CruP was only found in oxygenic phototrophs and only in conjunction with another lycopene β-cyclase. CruP was never found as the sole cyclase of any organism, whereas nonoxygenic phototrophs and nonphototrophs, as well as a few cyanobacteria, have only one lycopene cyclase (Dataset S2). This phylogenetic distribution of CruP, in comparison to other lycopene cyclases, suggests that either oxygenic photosynthesis has a requirement for more than one lycopene β-cyclase or that CruP has a function other than that of lycopene cyclization. The former hypothesis, that oxygenic photosynthetic organisms require more than one lycopene β-cyclase, seems unlikely because many cyanobacterial species have only one lycopene β-cyclase (either CrtL or CruA). Furthermore, this hypothesis does not explain the exclusion of CruP from all carotenoid-producing nonoxygenic organisms.

A phylogenetic tree was constructed based on 16S rRNA from fully sequenced cyanobacteria (Fig. 10). This tree identified evolutionarily distinct clades of cyanobacteria. One clade contained cyanobacteria with CruP, and another distinctly separate clade contained cyanobacteria that lacked CruP. The top clade (Fig. 10) was populated by open ocean cyanobacteria, encompassing all but two of the non–CruP-containing cyanobacteria. These open ocean cyanobacteria are also known as α-cyanobacteria, which are characterized by having a CO_2-concentrating mechanism involving a CsoS2 protein that is not found in β-cyanobacteria (36). Those cyanobacteria that contain CruP (bottom clade in Fig. 10) are from diverse ecological habitats, including fresh water, salt lakes, intertidal zones, hot springs, dry rocks, and symbiotic relationships, for example (36). These CruP-containing cyanobacteria, known as β-cyanobacteria, contain CO_2-concentrating mechanisms that use a CcmN protein not found in α-cyanobacteria (36). Cyanobacteria are able to exchange genetic material

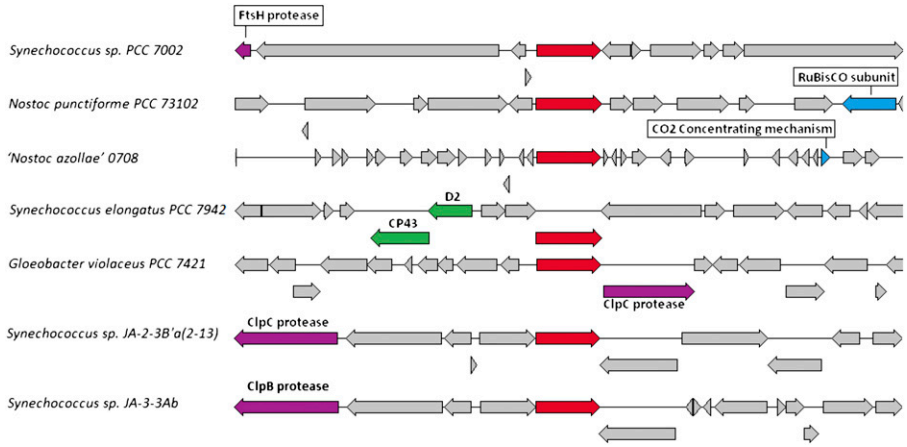

Fig. 11. CruP genes (red arrow) of select cyanobacteria show clustering with genes, the products of which are involved in carbon acquisition (blue arrows), the PSII reaction center (green arrows), and PSII reaction center repair (purple arrows).

via conjugation, and would therefore retain *cruP* in the genome if it provided an evolutionary advantage. This distribution suggests that CruP provides increased fitness to most β-cyanobacteria but not to α-cyanobacteria. β-cyanobacteria are exposed to variety of environmental extremes; in particular, temperature fluctuations (including chilling stress) and inorganic carbon limitations are two environmental conditions that β-cyanobacteria have to deal with but α-cyanobacteria do not (36). Chilling stress and low inorganic carbon are both conditions that lead to photoinhibition and to the up-regulation of *cruP* transcripts. Two cyanobacteria were noted as exceptions to the β-cyanobacterial distribution of CruP: *T. elongatus* and *cyanobacterium UCYN-A* are both β-cyanobacteria that lack CruP. *T. elongatus* is a thermophilic cyanobacterium isolated from Beppu hot springs in Japan, and this cyanobacterium reportedly has a reduced set of inorganic carbon transporters in comparison to other fresh water cyanobacteria (36). It is likely that the waters at this hot spring contain high levels of inorganic carbon attributable to mixing of volcanic CO_2, as has been reported for nearby thermal springs (49). As such, this cyanobacterium would not experience cold stress or inorganic carbon limitations in its natural environment, explaining the absence of CruP in this organism. *Cyanobacterium UCYN-A* is an unusual cyanobacterium with a reduced genome and no genes encoding PSII complex proteins or carbon fixation enzymes (50, 51). BLAST analysis revealed no genes with homology to CrtL, CruA, or CruP in the complete genome of this organism (Fig. 10), suggesting that another class of lycopene cyclase may exist and adding further evidence that CruP is not required in the absence of PSII (i.e., in nonoxygenic photosynthetic organisms).

Conclusions

We showed that absence of CruP was associated with increased ROS and increased β-carotene-5,6-epoxide, whereas overexpression of CruP was associated with reduced ROS, reduced β-carotene-5,6-epoxide, and a significantly reduced anthocyanin response under cold stress. The above results suggest that the function of CruP is to reduce oxidative damage caused by singlet oxygen. The above conclusion would explain the presence of β-carotene-5,6-epoxide, the anthocyanin response (or lack thereof in overexpressors) observed in cold-treated plants (Fig. 9), and the slow growth of the *Arabidopsis* mutant as well as the disordered thylakoid structure of the *Synechocystis cruP* KO (17). ROS generated by high excitation pressure of the photosystems during early development can cause a failure of chloroplasts to assemble organized internal structures (52). The lack of an observable difference in the pigment profile of cyanobacterial *cruP* KOs (8, 17), combined with the lack of lycopene cyclase activity of $_{Syn}$CruP in our study and the limited phylogenetic distribution of CruP, strongly suggests that CruP has a function other than lycopene cyclization. Considering the consistently observed up-regulation of *cruP* transcripts to photoinhibitory ROS-producing conditions, the limited phylogenetic distribution of CruP, and the inverse association between *cruP* transcript levels and ROS levels (and chemical markers of ROS levels), it appears that CruP plays a role, directly or indirectly, in reducing ROS levels in oxygenic photosynthetic organisms under photoinhibitory stress. Thus, CruP represents a unique target for developing resilient plants and algae needed to supply food and biofuels in the face of global climate change. The up-regulation of *cruP* during cold and anoxic conditions, such as flooding, suggests also that *cruP* will be an important locus to consider in screening for cold and submergence (anoxia) tolerance in plants.

Materials and Methods

Plasmids Used in This Study. Full details on plasmid construction are provided in *SI Materials and Methods*. pUC35S-$_{Zm}$CruP-GFP, pTNT-$_{Zm}$CruP-StrepTag, and pRed-$_{Zm}$CruP contained the full-length $_{Zm}$CruP transcript. p16-CPL1 and pET-$_{Syn}$CruP are pET16b-based vectors containing the *C. phaeobacteroides cruA* and *Synechococcus* sp. *PCC 7002 cruP* ORFs, respectively.

Bacterial Complementation Studies. *E. coli* BL21 (DE3) cells carrying plasmid pACCRT-EIB (12), which confers lycopene accumulation, were additionally transformed with either pET-$_{Syn}$CruP, p16-CPL1, or empty pET-16b as a negative control. Bacterial growth and extraction of carotenoids were performed as described previously (53) (*SI Materials and Methods*).

$_{At}$*cruP* KO and *35S:$_{Zm}$cruP* Lines. An *A. thaliana cruP* KO line (SALK_011725) carrying a T-DNA insert in the *cruP* gene in the Columbia background was obtained from The *Arabidopsis* Information Resource (20). Real-time PCR was performed to confirm the absence of *cruP* transcripts in the KO line as described below. For the generation of *35S:$_{Zm}$cruP*-overexpressing *A. thaliana* plants, *Agrobacterium tumefaciens* strain GV3101 (pMP90) was transformed with pRed-$_{Zm}$CruP using the freeze–thaw method (54) and selected using 50 μg/mL gentamicin and 50 μg/mL kanamycin. Floral dip transformation of *A. thaliana* was performed according to the method of Clough and Bent (55) (*SI Materials and Methods*). Transgenic seeds were selected using a pair of red-lens sunglasses (KD's Dark Red). Seeds that glowed red under a light of wavelength 550–560 nm were used in this study for overexpression experiments. Real-time PCR was performed to confirm overexpression as described previously (56). Primers 2617 and 2618 (Table S1) were used for amplification of actin cDNA, 1871 and 2190 (Table S1) for amplification of $_{Zm}$*cruP* cDNA, and 2978 and 2979 (Table S1) for amplification of $_{At}$*cruP* cDNA (*SI Materials and Methods*).

Standard Plant Growth Conditions. Unless otherwise stated, plants were grown in a Percival Scientific growth chamber under a 16-h day/8-h night cycle with a light intensity of 50 $\mu mol \cdot m^{-2} \cdot s^{-1}$ and a constant temperature of 21 °C. Plants were watered every 4 to 7 d.

Pigment Extraction and Analysis. Epoxy-5,6-β-carotene was synthesized according to the method of Barua (57) (*SI Materials and Methods*). Plant carotenoids were extracted by grinding roughly 30 mg of 4-wk-old plant tissue in 500 μL of 60:40 acetone/ethyl acetate; 400 μL of H_2O was added before vortexing and centrifugation for 5 min at 17,000 × *g*. The upper ethyl acetate fraction was washed, spun at 17,000 × *g* for 5 min, and then transferred to a different tube and dried under nitrogen before resuspension in methanol for HPLC analysis.

Separation of carotenoid and chlorophyll pigments was carried out using a Waters HPLC system equipped with a 2695 Alliance separation module, a 996-photodiode array detector, a Develosil C_{30} RP-Aqueous (5 μm, 250 mm × 4.6 mm) column (Phenomenex), and a Nucleosil C_{18} (5 μm, 4 mm × 3.0 mm) guard column (Phenomenex). Solvent A consisted of acetonitrile/methanol/H_2O (84:2:14), and solvent B consisted of methanol/ethyl acetate (68:32). Initial flow conditions consisted of 100% A at a flow rate of 0.6 mL/min. Using a linear gradient, flow was changed to 100% B by the 60-min mark; at this point, the flow rate was increased to 1.2 mL/min and held for an additional 50 min before being reequilibrated with A for 5 min. Column temperature was held at 30 °C, and 100 μL of each sample was injected for pigment analysis.

LC-MS was performed on a Waters 2695 HPLC machine equipped with a 2998 PDA detector coupled to a Waters LCT Premiere XE TOF MS system using electrospray ionization in positive ion mode.

Chloroplast Isolation and Protein Import. $_{Zm}$CruP was transcribed and translated in vitro from pTNT-$_{Zm}$CruP-StrepTag using SP6 polymerase in a rabbit reticulocyte lysate TnT-coupled system (Promega) in the presence of [^{35}S]methionine (PerkinElmer). Pea (*Pisum sativum*, var. Green Arrow; Jung Seed) plants were grown in a growth chamber, at 18–20 °C in a 14-h light/10-h dark cycle at 425 $\mu mol \cdot m^{-2} \cdot s^{-1}$. Plants were harvested and used for chloroplast isolation after 10–14 d as described previously (58) (*SI Materials and Methods*).

Protoplast Isolation and Transient Expression. Maize (*Z. mays* var. B73) mesophyll protoplasts were isolated from 10-d-old second leaves and transfected with the pUC35S-$_{Zm}$CruP-GFP vector, encoding a $_{Zm}$CruP-GFP fusion protein, by PEG-mediated transformation (59, 60) (*SI Materials and Methods*).

Phylogenetic/*in Silico* Analysis. The *Arabidopsis* Coexpression Data Mining Tools Web site (61) was used for analysis of genes that were coexpressed with $_{At}$*cruP* (At2g32640) and the gene encoding $_{At}$LCYE (At5g57030). The Rice Oligonucleotide Array Database (62) Web site was used for analysis of genes that were coexpressed with $_{Os}$*cruP* (Os8g32630). Genevestigator (63) was used for analyzing variation of $_{At}$*cruP* transcript levels under different conditions and in various tissues. The SEED database (64) was used for analysis of genes that clustered with cyanobacterial *cruP* genes.

The results of a protein BLAST search using the *Synechococcus* sp. *PCC 7002* CruP protein sequence were compared with the results of a protein BLAST search of the *Synechococcus* sp. *PCC 7002* CruA protein sequence. Only results with an E-value greater than 0.005 (the standard BLAST cutoff score) were used. Those proteins that had a smaller E-value in the CruP set were considered CruP orthologs; the others were considered CruA orthologs.

16S rRNA sequences from cyanobacteria with complete genomes were obtained from National Center for Biotechnology Information genomes (http://www.ncbi.nlm.nih.gov/genome) aligned using ClustalW2 (European Bioinformatics Institute; http://www.ebi.ac.uk/Tools/msa/clustalw2/). Alignments were then imported into MEGA 5.05 (65) for construction of a neighbor-joining tree with 1,000 replications for bootstrap values.

ROS Analysis. Seeds were sterilized in 1 mL of 70% ethanol for 5 min, followed by 5 min in 1 mL of 25% bleach solution containing 0.01% Tween 100. The bleach solution was removed, and seeds were rinsed five times with sterile milliQ H_2O. The seeds were soaked under 900 μL of sterile milliQ H_2O (to create a photoinhibitory environment) and placed at 4 °C for 2 d before being placed at a 21 °C 14-h light/10-h dark cycle for 2 wk. Plants were stained with 2 mM NTB in 20 mM phosphate buffer (pH 6.1) for 15 min (66). Reactions were stopped by removing the NTB solution and flushing with sterile distilled water.

ACKNOWLEDGMENTS. We thank Dr. Edgar Cahoon (University of Nebraska, Lincoln) for the pBin35SRed vector, Dr. Donald Bryant (Pennsylvania State University) for the $_{Cp}$CruA-containing vector p16-CPL1, and Dr. Abby Cuttriss for her helpful insights and discussion. Financial support is acknowledged from National Institutes of Health Grant GM081160 (to E.T.W.) and National Institutes of Health-National Heart, Lung, and Blood Institute Grant 5SC1HL096016 (to E.J.K.).

1. Namitha KK, Negi PS (2010) Chemistry and biotechnology of carotenoids. *Crit Rev Food Sci Nutr* 50:728–760.
2. Fedtke C, et al. (2001) Mode of action of new diethylamines in lycopene cyclase inhibition and in photosystem II turnover. *Pest Manag Sci* 57:278–282.
3. La Rocca N, Rascio N, Oster U, Rüdiger W (2007) Inhibition of lycopene cyclase results in accumulation of chlorophyll precursors. *Planta* 225:1019–1029.
4. Cuttriss AJ, Cazzonelli CI, Wurtzel ET, Pogson BJ (2011) Carotenoids. *Biosynthesis of Vitamins in Plants, Advances in Botanical Research*, eds Rébeillé F, Douce R (Elsevier, Amsterdam), pp 1–36.
5. Cunningham FX, Jr., et al. (1996) Functional analysis of the beta and epsilon lycopene cyclase enzymes of Arabidopsis reveals a mechanism for control of cyclic carotenoid formation. *Plant Cell* 8:1613–1626.
6. Iniesta AA, Cervantes M, Murillo FJ (2008) Conversion of the lycopene monocyclase of Myxococcus xanthus into a bicyclase. *Appl Microbiol Biotechnol* 79:793–802.
7. Krubasik P, Sandmann G (2000) Molecular evolution of lycopene cyclases involved in the formation of carotenoids with ionone end groups. *Biochem Soc Trans* 28: 806–810.
8. Maresca JA, Graham JE, Wu M, Eisen JA, Bryant DA (2007) Identification of a fourth family of lycopene cyclases in photosynthetic bacteria. *Proc Natl Acad Sci USA* 104: 11784–11789.
9. Pogson B, McDonald KA, Truong M, Britton G, DellaPenna D (1996) Arabidopsis carotenoid mutants demonstrate that lutein is not essential for photosynthesis in higher plants. *Plant Cell* 8:1627–1639.
10. Telfer A (2002) What is beta-carotene doing in the photosystem II reaction centre? *Philos Trans R Soc Lond B Biol Sci* 357:1431–1439, discussion 1439–1440, 1469–1470.
11. Telfer A (2005) Too much light? How beta-carotene protects the photosystem II reaction centre. *Photochem Photobiol Sci* 4:950–956.
12. Cunningham FX, Jr., Chamovitz D, Misawa N, Gantt E, Hirschberg J (1993) Cloning and functional expression in Escherichia coli of a cyanobacterial gene for lycopene cyclase, the enzyme that catalyzes the biosynthesis of beta-carotene. *FEBS Lett* 328: 130–138.
13. Cunningham FX, Jr., Sun Z, Chamovitz D, Hirschberg J, Gantt E (1994) Molecular structure and enzymatic function of lycopene cyclase from the cyanobacterium Synechococcus sp strain PCC7942. *Plant Cell* 6:1107–1121.
14. Yu Q, et al. (2010) The lycopene cyclase CrtY from *Pantoea ananatis* (formerly *Erwinia uredovora*) catalyzes an FADred-dependent non-redox reaction. *J Biol Chem* 285: 12109–12120.
15. Krubasik P, Sandmann G (2000) A carotenogenic gene cluster from *Brevibacterium linens* with novel lycopene cyclase genes involved in the synthesis of aromatic carotenoids. *Mol Gen Genet* 263:423–432.
16. Velayos A, Eslava AP, Iturriaga EA (2000) A bifunctional enzyme with lycopene cyclase and phytoene synthase activities is encoded by the *carRP* gene of *Mucor circinelloides*. *Eur J Biochem* 267:5509–5519.
17. Liang C-W, Zhang X-W, Tian L, Qin S (2008) Functional characterization of *sll0659* from Synechocystis sp. PCC 6803. *Indian J Biochem Biophys* 45:275–277.
18. Meier S, Tzfadia O, Vallabhaneni R, Gehring C, Wurtzel ET (2011) A transcriptional analysis of carotenoid, chlorophyll and plastidial isoprenoid biosynthesis genes during development and osmotic stress responses in *Arabidopsis thaliana*. *BMC Syst Biol* 5:77.
19. Robertson D, Anderson I, Bachmann M (1978) Pigment-deficient mutants: Genetic, biochemical and developmental studies. *Maize Breeding and Genetics*, ed Walden D (John Wiley & Sons, New York), pp 461–494.
20. Swarbreck D, et al. (2008) The Arabidopsis Information Resource (TAIR): Gene structure and function annotation. *Nucleic Acids Res* 36(Database issue):D1009–D1014.
21. Ashikawa I, et al. (1987) All-trans β-carotene-5, 6-epoxide in thylakoid membranes. *Photochem Photobiol* 46:269–275.
22. Bungard RA, et al. (1999) Unusual carotenoid composition and a new type of xanthophyll cycle in plants. *Proc Natl Acad Sci USA* 96:1135–1139.
23. Cunningham FX, Jr., Gantt E (2011) Elucidation of the pathway to astaxanthin in the flowers of *Adonis aestivalis*. *Plant Cell* 23:3055–3069.
24. Zepka LQ, Mercadante AZ (2009) Degradation compounds of carotenoids formed during heating of a simulated cashew apple juice. *Food Chem* 117:28–34.
25. Berset C, Marty C (1992) Formation of nonvolatile compounds by thermal-degradation of beta-carotene—Protection by antioxidants. *Methods Enzymol* 213: 129–142.
26. Sun X, et al. (2007) Formation of DEG5 and DEG8 complexes and their involvement in the degradation of photodamaged photosystem II reaction center D1 protein in Arabidopsis. *Plant Cell* 19:1347–1361.
27. Sakamoto W, Tamura T, Hanba-Tomita Y, Murata M; Sodmergen (2002) The *VAR1* locus of Arabidopsis encodes a chloroplastic FtsH and is responsible for leaf variegation in the mutant alleles. *Genes Cells* 7:769–780.
28. Liu X, Rodermel SR, Yu F (2010) A *var2* leaf variegation suppressor locus, *SUPPRESSOR OF VARIEGATION3*, encodes a putative chloroplast translation elongation factor that is important for chloroplast development in the cold. *BMC Plant Biol* 10:287.

29. Ishihara S, et al. (2007) Distinct functions for the two PsbP-like proteins PPL1 and PPL2 in the chloroplast thylakoid lumen of Arabidopsis. *Plant Physiol* 145:668–679.
30. Mochizuki N, Brusslan JA, Larkin R, Nagatani A, Chory J (2001) Arabidopsis *genomes uncoupled 5* (*GUN5*) mutant reveals the involvement of Mg-chelatase H subunit in plastid-to-nucleus signal transduction. *Proc Natl Acad Sci USA* 98:2053–2058.
31. Renné P, et al. (2003) The Arabidopsis mutant *dct* is deficient in the plastidic glutamate/malate translocator DiT2. *Plant J* 35:316–331.
32. Howles PA, et al. (2006) A mutation in an Arabidopsis ribose 5-phosphate isomerase reduces cellulose synthesis and is rescued by exogenous uridine. *Plant J* 48:606–618.
33. Raynaud C, Cassier-Chauvat C, Perennes C, Bergounioux C (2004) An Arabidopsis homolog of the bacterial cell division inhibitor SulA is involved in plastid division. *Plant Cell* 16:1801–1811.
34. Suorsa M, et al. (2010) Two proteins homologous to PsbQ are novel subunits of the chloroplast NAD(P)H dehydrogenase. *Plant Cell Physiol* 51:877–883.
35. Yabuta S, et al. (2010) Three PsbQ-like proteins are required for the function of the chloroplast NAD(P)H dehydrogenase complex in Arabidopsis. *Plant Cell Physiol* 51: 866–876.
36. Badger MR, Price GD, Long BM, Woodger FJ (2006) The environmental plasticity and ecological genomics of the cyanobacterial CO2 concentrating mechanism. *J Exp Bot* 57:249–265.
37. Fiedor J, Fiedor L, Winkler J, Scherz A, Scheer H (2001) Photodynamics of the bacteriochlorophyll-carotenoid system. 1. Bacteriochlorophyll-photosensitized oxygenation of beta-carotene in acetone. *Photochem Photobiol* 74:64–71.
38. Nixon PJ, Michoux F, Yu J, Boehm M, Komenda J (2010) Recent advances in understanding the assembly and repair of photosystem II. *Ann Bot (Lond)* 106:1–16.
39. Krieger-Liszkay A, Fufezan C, Trebst A (2008) Singlet oxygen production in photosystem II and related protection mechanism. *Photosynth Res* 98:551–564.
40. Trebst A, Depka B (1997) Role of carotene in the rapid turnover and assembly of photosystem II in *Chlamydomonas reinhardtii*. *FEBS Lett* 400:359–362.
41. La Rocca N, Barbato R, Casadoro G, Rascio N (1996) Early degradation of photosynthetic membranes in carob and sunflower cotyledons. *Physiol Plant* 96: 513–518.
42. Yiotis C, Manetas Y (2010) Sinks for photosynthetic electron flow in green petioles and pedicels of *Zantedeschia aethiopica*: Evidence for innately high photorespiration and cyclic electron flow rates. *Planta* 232:523–531.
43. Wilson KE, Huner NP (2000) The role of growth rate, redox-state of the plastoquinone pool and the trans-thylakoid deltapH in photoacclimation of *Chlorella vulgaris* to growth irradiance and temperature. *Planta* 212:93–102.
44. Wilson KE, Król M, Huner NPA (2003) Temperature-induced greening of *Chlorella vulgaris*. The role of the cellular energy balance and zeaxanthin-dependent nonphotochemical quenching. *Planta* 217:616–627.
45. Allen DJ, Ort DR (2001) Impacts of chilling temperatures on photosynthesis in warm-climate plants. *Trends Plant Sci* 6:36–42.
46. Blokhina O, Fagerstedt KV (2010) Oxidative metabolism, ROS and NO under oxygen deprivation. *Plant Physiol Biochem* 48:359–373.
47. Blokhina OB, Chirkova TV, Fagerstedt KV (2001) Anoxic stress leads to hydrogen peroxide formation in plant cells. *J Exp Bot* 52:1179–1190.
48. Zhu Y, et al. (2010) Roles of xanthophyll carotenoids in protection against photoinhibition and oxidative stress in the cyanobacterium Synechococcus sp. strain PCC 7002. *Arch Biochem Biophys* 504:86–99.
49. Yamada M, et al. (2011) Mixing of magmatic CO_2 into volcano groundwater flow at Aso volcano assessed combining carbon and water stable isotopes. *J Geochem Explor* 108:81–87.
50. DeLong EF (2010) Interesting things come in small packages. *Genome Biol* 11(5):1–4.
51. Tripp HJ, et al. (2010) Metabolic streamlining in an open-ocean nitrogen-fixing cyanobacterium. *Nature* 464:90–94.
52. McDonald AE, et al. (2011) Flexibility in photosynthetic electron transport: The physiological role of plastoquinol terminal oxidase (PTOX). *Biochim Biophys Acta* 1807:954–967.
53. Quinlan RF, Jaradat TT, Wurtzel ET (2007) Escherichia coli as a platform for functional expression of plant P450 carotene hydroxylases. *Arch Biochem Biophys* 458:146–157.
54. Seetharam R, Sridhar K (2007) A modified freeze–thaw method for efficient transformation of *Agrobacterium tumefaciens*. *Curr Sci* 93:770–772.
55. Clough SJ, Bent AF (1998) Floral dip: A simplified method for Agrobacterium-mediated transformation of *Arabidopsis thaliana*. *Plant J* 16:735–743.
56. Vallabhaneni R, Bradbury LMT, Wurtzel ET (2010) The carotenoid dioxygenase gene family in maize, sorghum, and rice. *Arch Biochem Biophys* 504:104–111.
57. Barua AB (1999) Intestinal absorption of epoxy-beta-carotenes by humans. *Biochem J* 339:359–362.
58. Bruce BD, Perry S, Froehlich J, Keegstra K (1994) In vitro import of protein into chloroplasts. *Plant Molecular Biology Manual*, ed Gelvin SB, Schilperoort RA (Kluwer, Boston), Vol J1, pp 1–15.
59. Sheen J (1991) Molecular mechanisms underlying the differential expression of maize pyruvate, orthophosphate dikinase genes. *Plant Cell* 3:225–245.
60. van Bokhoven H, Verver J, Wellink J, van Kammen A (1993) Protoplasts transiently expressing the 200K coding sequence of cowpea mosaic virus B-RNA support replication of M-RNA. *J Gen Virol* 74:2233–2241.
61. Manfield IW, et al. (2006) Arabidopsis Co-expression Tool (ACT): Web server tools for microarray-based gene expression analysis. *Nucleic Acids Res* 34(Web Server issue): W504–W509.
62. Jung KH, et al. (2008) Refinement of light-responsive transcript lists using rice oligonucleotide arrays: Evaluation of gene-redundancy. *PLoS ONE* 3:e3337.
63. Hruz T, et al. (2008) Genevestigator V3: A reference expression database for the meta-analysis of transcriptomes. *Adv Bioinformatics* 2008:420747.
64. Overbeek R, et al. (2005) The subsystems approach to genome annotation and its use in the project to annotate 1000 genomes. *Nucleic Acids Res* 33:5691–5702.
65. Tamura K, et al. (2011) MEGA5: Molecular evolutionary genetics analysis using maximum likelihood, evolutionary distance, and maximum parsimony methods. *Mol Biol Evol* 28:2731–2739.
66. Kato Y, Miura E, Ido K, Ifuku K, Sakamoto W (2009) The variegated mutants lacking chloroplastic FtsHs are defective in D1 degradation and accumulate reactive oxygen species. *Plant Physiol* 151:1790–1801.

Supporting Information

Bradbury et al. 10.1073/pnas.1206002109

SI Materials and Methods

Plasmids Used in This Study. *Zea mays cruP* (*$_{Zm}$cruP*) cDNA clone (clone ID ZM_BFc0139E12) pSPORT-$_{Zm}$CruP was ordered from the Arizona Genomics Institute. Using BamHI and EcoRI, the gene encoding GFP was cut from pBIG121 (1) and cloned into the same sites of pUC35S-GUS-Nos (1) to generate pUC35S-sGFP-Nos. *$_{Zm}$cruP* was PCR-amplified from pSPORT-$_{Zm}$CruP using primers 2487 and 2938 (Table S1) to incorporate XbaI and BamHI restriction enzyme sites, respectively. The PCR product and pUC35S-sGFP-Nos were digested with XbaI and BamHI before ligation to generate the plasmid pUC35S-$_{Zm}$CruP-GFP for use in transient expression studies. For protein import studies, ZmCruP was amplified from pSPORT-$_{Zm}$CruP using primers 2960 and 2958, digested with Xho1 and Xba1, and inserted into these sites of the pTNT vector (Promega), giving the vector pTNT-$_{Zm}$CruP-StrepTag. *$_{Zm}$cruP* was PCR-amplified from pSPORT-$_{Zm}$CruP using primers 2487 and 2930 (Table S1) to incorporate two XbaI restriction enzyme sites. The PCR product and pBin35SRed (2), containing a 35S promoter to drive expression of the transgene, were digested with XbaI before ligation to generate the plasmid pRed-$_{Zm}$CruP for use in *Arabidopsis* stable transformation. The $_{Cp}$CruA plasmid (p16-CPL1) (3) was used as a positive control. *Synechococcus* sp. *PCC 7002 cruP* (*$_{Syn}$cruP*) ORF (NC_010475) was synthesized and cloned into pUC57 by GenScript to generate pUC-$_{Syn}$cruP. *$_{Syn}$cruP* was PCR-amplified from pUC-$_{Syn}$cruP using primers 2986 and 2987 (Table S1) to incorporate an NdeI site upstream of the start codon and a BamHI site downstream of the stop codon. After digestion of this PCR product and of pET16b (Novagen) with these restriction enzymes, *$_{Syn}$cruP* was ligated into pET16b to generate pET-$_{Syn}$CruP, used for in vitro studies.

Bacterial Complementation and Pigment Analysis. For carotenoid analyses, saturated cultures in LB were diluted 100-fold into 50 mL of fresh medium in 250-mL flasks and were grown in the dark at 250 rpm (Innova 4080 shaker; New Brunswick Scientific) at 37 °C until OD_{600} = 0.5; at that point, they were induced with 5 mM isopropyl-β-D-thiogalactopyranoside and further cultured for a total of 3 d at 28 °C. For extraction of carotenoids produced in bacteria, bacterial cultures were centrifuged at 2,000 × *g* for 10 min at 4 °C, the supernatant was removed, and 5 mL of 50:50 methanol/acetone was added to the bacterial pellet before vigorously vortexing. The sample was again centrifuged at 2,000 × *g* for 10 min at 4 °C, and the supernatant was transferred to a different tube. The sample was dried down under nitrogen and resuspended in 500 μL of 60:40 acetone/ethyl acetate; 400 μL of H_2O was added before vortexing and centrifugation for 5 min at 17,000 × *g*. The upper ethyl acetate fraction was transferred to a different tube, spun at 17,000 × *g* for 5 min, and again transferred to another tube before being dried down under nitrogen and resuspended in methanol for HPLC analysis.

Generation of 35S:$_{Zm}$cruP Lines Segregating Populations. *Agrobacterium tumefaciens* strain GV3101 (pMP90) was transformed with pRed-$_{Zm}$CruP using the freeze–thaw method (4) and selected using 50 μg/mL gentamicin and 50 μg/mL kanamycin. Floral dip transformation of *Arabidopsis thaliana* was performed according to the method of Clough and Bent (5) as described below. A single *Agrobacterium* colony was grown overnight in 20 mL of LB with 50 μg/mL gentamicin and 50 μg/mL kanamycin. Four milliliters of overnight culture was transferred to 400 mL of LB and grown to OD_{600} = 0.8. *Agrobacterium* cells were pelleted by centrifugation at 1,500 × *g* at 4 °C for 15 min before being resuspended in 700 mL of 5% sucrose plus 0.05% silwet 77 (Lehle Seeds). Plant flowers were soaked in the *Agrobacterium* solution for 45 s, placed in a tray lined with wet paper towels, covered to maintain high humidity, and then placed in the dark for 12–16 h. Plants were taken out to air-dry before returning them to standard growth conditions (below). Plants were watered for 3 wk and then left to dry out before seeds were collected. Segregating populations were generated by transferring pollen from *$_{At}$cruP* KO plants to the stigma of WT Columbia plants and also by transferring pollen from *$_{At}$cruP* KO plants to the stigma of *35S:$_{Zm}$cruP* plants. Primers 2292 and 2293 (Table S1) were used to screen for plants with no T-DNA insert in the *$_{At}$cruP* gene, and the primers 2292 and 1857 (Table S1) were used to screen for the presence of a T-DNA insert of the *$_{At}$cruP* gene. Transgenic *35S:$_{Zm}$cruP*-overexpressing plants were selected at the seed stage as described above.

Real-Time PCR. For real-time PCR, total RNA was isolated from *Arabidopsis* lines using the RNeasy Plant Mini Kit (Qiagen) and then treated with DNase I according to the manufacturer's instructions (Invitrogen). First-strand cDNA synthesis was carried out using an oligo (dT) primer and SuperScript III RT (Invitrogen) according to the manufacturer's instructions. Ten nanograms of cDNA was used for each real-time PCR assay, and samples were amplified using a SYBR GreenER Supermix (Bio-Rad). Thermal cycling conditions in a MyIQ Single-Color Real-Time PCR detection system (Bio-Rad) included an initial incubation at 94 °C for 10 s, followed by 35 cycles of 95 °C for 10 s, 58 °C for 35 s, and 72 °C for 10 s. The relative quantity of the transcripts was calculated using the comparative threshold cycle method (6). Actin2 (AT3G18780) was used as a standard for normalization between samples. Three technical replicates of each experiment were performed.

β-Carotene-5,6-Epoxide Synthesis. β-carotene-5,6-epoxide was synthesized according to the method of Berset and Marty (7). β-carotene was mixed with 0.3× molar concentrations of M-chloroperbenzoic acid in diethyl ether and stirred at 4 °C for 1 h. This solution was then mixed with equal parts of water containing dilute NaOH before centrifugation at 17,000 × *g* for 5 min. The top diethyl ether fraction was transferred to a different tube, washed with water, and spun, and the diethyl ether fraction was transferred to a different tube before being dried down under nitrogen and redissolved in methanol for HPLC analysis.

Chloroplast Isolation and Protein Import. Pea (*Pisum sativum*, var. Green Arrow; Jung Seed) plants were grown in a growth chamber at 18–20 °C in a 14-h/10-h dark/light cycle at 425 $\mu mol \cdot m^{-2} \cdot s^{-1}$. Plants were harvested and used for chloroplast isolation after 10–14 d as described previously (8). To prevent starch accumulation, plant leaves were collected after 8 h of dark and then ground with a kitchen blender in a grinding buffer [50 mM Hepes (pH 8), 330 mM sorbitol, 1 mM $MnCl_2$, 1 mM $MgCl_2$, 2 mM EDTA, 0.2% wt/vol BSA, 0.1% wt/vol ascorbic acid] at 4 °C. Chloroplasts were isolated using Percoll gradient centrifugation (8). The Percoll gradient was prepared by centrifugation of 50% Percoll (Sigma) in the grinding buffer (40,000 × *g* for 30 min at 4 °C). Chloroplast suspension was layered on the top of the gradient and centrifuged at 12,000 × *g* for 10 min. The lower band, containing intact chloroplasts, was aspirated and washed with the import buffer [50 mM Hepes (pH 8), 330 mM sorbitol]. Intact chloroplasts were resuspended in 140 μL per reaction of import mix [50 mM Hepes

(pH 8), 330 mM sorbitol, 4 mM methionine, 4 mM ATP, 4 mM $MgCl_2$, 10 mM K-Ac, 10 mM $NaHCO_3$] at a concentration 50 μg of chlorophyll per reaction. For the import reaction, 10 μL of in vitro transcription/translation product was added to the chloroplast mix. After 25 min at 25 °C in the light, the import reaction was stopped by placing on ice and diluting with 500 μL of cold import buffer. Chloroplasts were collected by centrifugation (800 × *g* for 2 min), diluted in 200 μL of fresh cold import buffer, supplemented with 1 mM $CaCl_2$, and divided into two parts; one was left intact, and the other was treated with 125 ng/μL thermolysin for 30 min on ice. The reaction was stopped by adding EDTA to a final concentration of 10 mM. Chloroplasts were collected by centrifugation at 800 × *g* for 2 min. Sample buffer for SDS/PAGE was added to the pellets, and the protein extracts were analyzed by gel electrophoresis. For fractionation after import, intact chloroplasts were washed two times with import buffer and then diluted with HL buffer [10 mM Hepes·KOH, 10 mM $MgCl_2$ (pH 8)]. The total mixture was frozen in liquid nitrogen and thawed three times and then centrifuged at 16,000 × *g* for 20 min. Supernatant, containing soluble chloroplast proteins, and the pellet, containing membrane fraction, were analyzed by means of an SDS/PAGE gel. Alkaline treatment of the membrane fraction was performed with 200 mM Na_2CO_3 for 10 min on ice. Membranes were separated from supernatant by centrifugation at 16,000 × *g* for 20 min and analyzed by SDS/PAGE. Radiolabeled protein was analyzed by phosphorimaging (Storm; Molecular Dynamics).

Protoplast Isolation and Transient Expression. Isolation and transformation of maize protoplasts were performed according to classic protocols (9, 10) with modifications. Maize var. B73 plants were grown in the dark at 26 °C for 12 d (Avantis growth chamber; Conviron). Middle parts of the second leaves of 20 plants were cut into razor-thin sections and transferred to a 500-mL Erlenmeyer flask containing 50 mL of Ca/mannitol solution [10 mM $CaCl_2$, 0.6 M mannitol, 20 mM Mes (pH 5.7)] to which was added 1% cellulase (*Trichoderma viride*), 0.3% pectinase (*Rhizopus* sp.; Sigma), 5 mM β-mercaptoethanol (Sigma), and 0.1% BSA (Sigma). A vacuum was applied for 5 min, followed by shaking at 60 rpm (Innova 4080 shaker; New Brunswick Scientific) at room temperature in the dark for 3 h. The supernatant was filtered using a 60-μm nylon mesh, collected in a 50-mL Falcon centrifuge tube by centrifugation at 500 × *g*, and then washed three times with Ca/mannitol solution [0.6 M mannitol, 10 mM $CaCl_2$, 20 mM Mes (pH 5.6)]. Purified pUC35S-$_{Zm}$CruP-GFP plasmid DNA (10 μg in 25 μL of ice-cold water) was added to 1×10^6 protoplasts in 100 μL of ice-cold 0.6 M mannitol containing 10 mM $CaCl_2$ and immediately diluted with 500 μL of PEG solution [40% PEG 6000, 0.5 M mannitol, 0.1 M $Ca(NO_3)_2$]. The protoplast suspension was gently mixed for 10–15 s, diluted with 4.5 mL of mannitol/Mes solution [0.5 M mannitol, 15 mM $MgCl_2$, 0.1% Mes (pH 5.6)], and kept at room temperature for 20 min. The protoplasts were centrifuged at 500 × *g* for 5 min at room temperature, the supernatant was removed, and the pellet was resuspended in 1 mL of Ca/mannitol solution and incubated for 12–16 h at 25 °C. Transient expression of the $_{Zm}$CruP:GFP fusion protein was visualized with a DMI6000B inverted confocal microscope with a TCS SP5 system (Leica Microsystems CMS) using a water immersion objective (63×). A 488-nm argon laser was used as the excitation wavelength of GFP and chlorophyll. The chloroplast autofluorescence was detected between 664 and 696 nm, and the GFP fluorescence was detected between 500 and 539 nm and always confirmed by recording the emission spectrum by wavelength scanning (λ-scan) between 500 and 600 nm with a 3-nm detection window. LAS AF software (Leica Microsystems CMS) was used for image acquisition. Images were obtained by combining several confocal Z- planes that had each been subjected to deconvolution.

1. Okada K, Saito T, Nakagawa T, Kawamukai M, Kamiya Y (2000) Five geranylgeranyl diphosphate synthases expressed in different organs are localized into three subcellular compartments in Arabidopsis. *Plant Physiol* 122:1045–1056.
2. Yang W, et al. (2011) Vitamin E biosynthesis: Functional characterization of the monocot homogentisate geranylgeranyl transferase. *Plant J* 65:206–217.
3. Maresca JA, Romberger SP, Bryant DA (2008) Isorenieratene biosynthesis in green sulfur bacteria requires the cooperative actions of two carotenoid cyclases. *J Bacteriol* 190:6384–6391.
4. Seetharam R, Sridhar K (2007) A modified freeze–thaw method for efficient transformation of *Agrobacterium tumefaciens*. *Curr Sci* 93:770–772.
5. Clough SJ, Bent AF (1998) Floral dip: A simplified method for Agrobacterium-mediated transformation of *Arabidopsis thaliana*. *Plant J* 16:735–743.
6. Vallabhaneni R, Bradbury LMT, Wurtzel ET (2010) The carotenoid dioxygenase gene family in maize, sorghum, and rice. *Arch Biochem Biophys* 504:104–111.
7. Berset C, Marty C (1992) Formation of nonvolatile compounds by thermal-degradation of beta-carotene—Protection by antioxidants. *Methods Enzymol* 213:129–142.
8. Bruce BD, Perry S, Froehlich J, Keegstra K (1994) In vitro import of protein into chloroplasts. *Plant Molecular Biology Manual*, ed Gelvin SB, Schilperoot RA (Kluwer, Boston), Vol J1, pp 1–15.
9. Sheen J (1991) Molecular mechanisms underlying the differential expression of maize pyruvate, orthophosphate dikinase genes. *Plant Cell* 3:225–245.
10. van Bokhoven H, Verver J, Wellink J, van Kammen A (1993) Protoplasts transiently expressing the 200K coding sequence of cowpea mosaic virus B-RNA support replication of M-RNA. *J Gen Virol* 74:2233–2241.

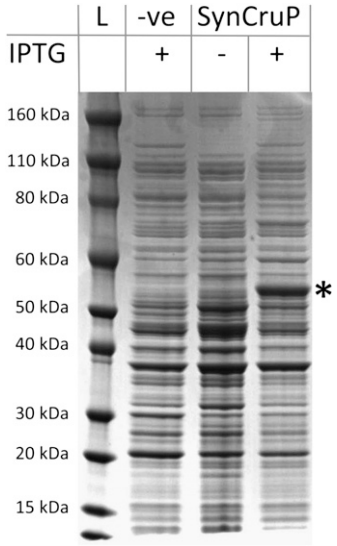

Fig. S1. SDS/PAGE image shows Unstained Novex Sharp Ladder (L; Invitrogen), empty pET16b plasmid induced with 1 mM isopropyl-β-D-thiogalactopyranoside (IPTG; −ve), and (SynCruP) without (–) and with (+) induction by 1 mM IPTG. The asterisk corresponds to the band of expected size for CruP (~57 kDa). All protein extracts are from *Escherichia coli* BL21 cells expressing a plasmid for lycopene accumulation as well as the respective plasmid listed above.

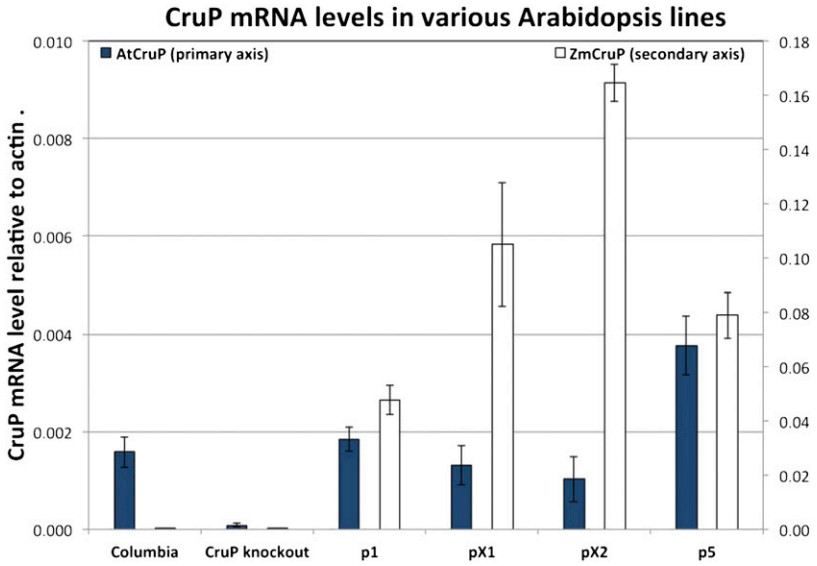

Fig. S2. Transcript levels of $_{At}$*cruP* (blue, primary *y* axis) and $_{Zm}$*cruP* (white, secondary *y* axis) in six *Arabidopsis* lines (Columbia, $_{At}$*cruP* KO, and four *35S*:$_{Zm}$cruP lines) in comparison to the *actin2* standard as determined by real-time PCR.

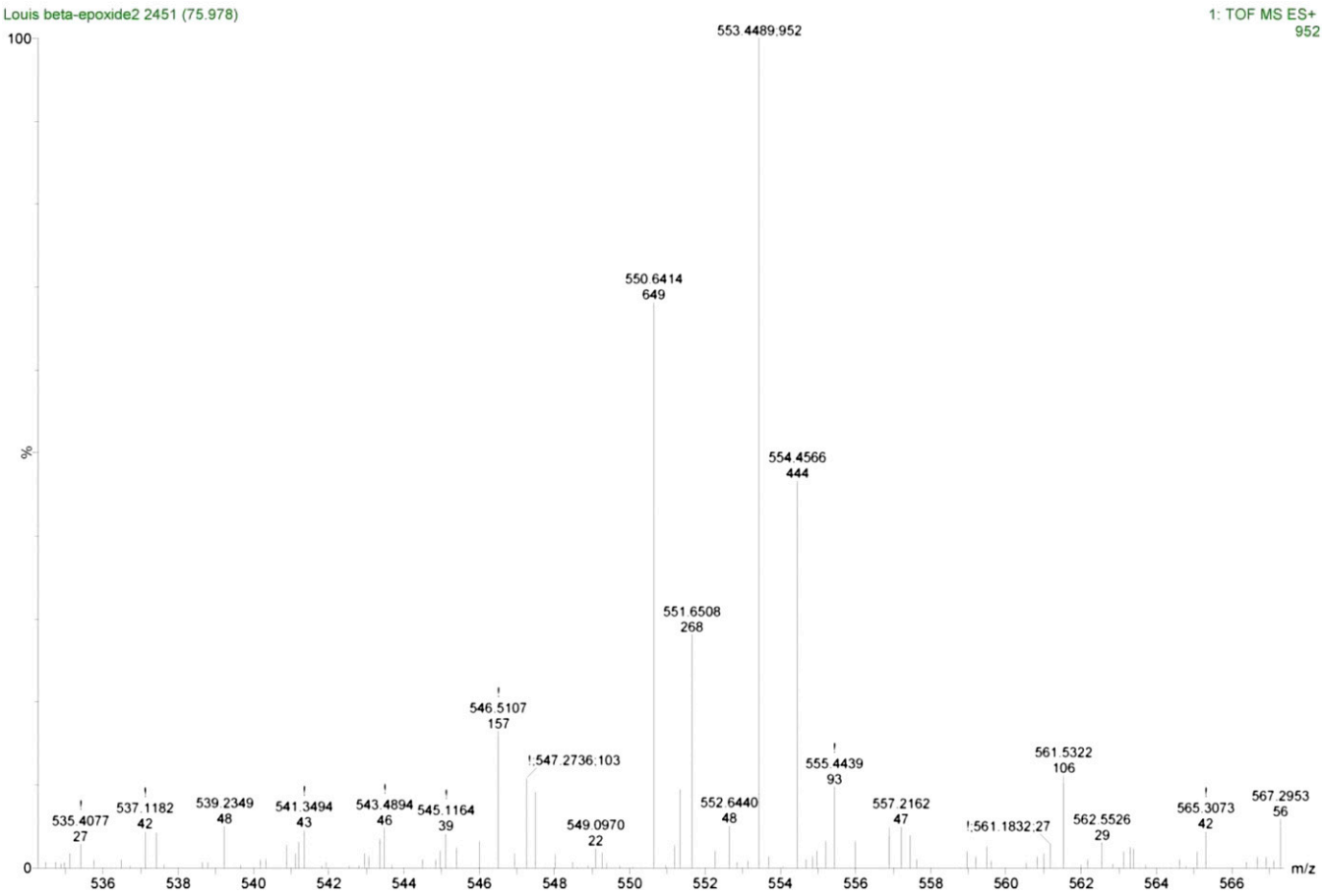

Fig. S3. Liquid chromatography-MS fragments obtained from the peak corresponding to β-carotene-5,6-epoxide (positive mode).

Table S1. Primers used in this study

Name	Sequence 5′-3′
1857	TGGTTCACGTAGTGGGCCATCG
1871	ATTCCAAAGTCCCTGAAGTTGTTAC
2190	ATATTCCACTCCTGTTCCCTCCCT
2292	TTGCGTCATAGATTCCTTTT
2293	ACTTGTCACCAGTCCGTTGC
2487	ACTCTAGATGCCTCCGCCT
2617	GAGCGACAACCCGAAGACC
2618	AATCCATATGGAATCCCTAGC
2930	GATCTAGATTATTCCCCTTGGCGGTAATC
2938	GAGGATCCTTCCCCTTGGCGGTAATC
2958	GTCTCTAGATTATTTTTCAAATTGAGGATGAGACCATTCCCCTTGGCGGTAATCTAAACCG
2960	ACTCGAGATGCCTCCGCCTGTTCTTC
2965	GATTCTAGATGCCTCCGCCTGTTCTT
2978	GGCTCTGGTCCATTAGACCGCA
2979	GCAGCTGGCAACGGACTATTTCG
2986	TATCGGACATATGGGTCAGG
2987	CGGGATCCAAGCTTAGTCCTGTTC

Dataset S1. Genes coexpressed with genes encoding $_{At}$CruP (*A*), $_{At}$CruP and $_{Os}$CruP (*B*), and $_{At}$LCYE (*C*). Column 1 shows genes of interest in green (photosystem related), red (repair or protection from ROS), and blue (inorganic carbon acquisition/fixation)

Dataset S1 (XLSX)

Coexpression data obtained from *Arabidopsis* Coexpression Data Mining Tools; gene descriptions obtained from The *Arabidopsis* Information Resource.

Dataset S2. Detailed phylogenetic distribution of CruA, CrtY, and CrtL type cyclases and of CruP proteins showing species name and GenBank protein accession number for each

Dataset S2 (XLSX)

Details of completion of genome sequence are also shown.